

## Substrate-Insensitive Phased Array with Improved Circularly-Polarized Scan Angle for 5G Mobile Terminals

Zhang, Shuai; Syrytsin, Igor A.; Pedersen, Gert F.

*Published in:*  
12th European Conference on Antenna and Propagation (EUCAP 2018)

*DOI (link to publication from Publisher):*  
[10.1049/cp.2018.0421](https://doi.org/10.1049/cp.2018.0421)

*Publication date:*  
2018

*Document Version*  
Accepted author manuscript, peer reviewed version

[Link to publication from Aalborg University](#)

*Citation for published version (APA):*  
Zhang, S., Syrytsin, I. A., & Pedersen, G. F. (2018). Substrate-Insensitive Phased Array with Improved Circularly-Polarized Scan Angle for 5G Mobile Terminals. In *12th European Conference on Antenna and Propagation (EUCAP 2018)* Institution of Engineering and Technology (IET).  
<https://doi.org/10.1049/cp.2018.0421>

### General rights

Copyright and moral rights for the publications made accessible in the public portal are retained by the authors and/or other copyright owners and it is a condition of accessing publications that users recognise and abide by the legal requirements associated with these rights.

- Users may download and print one copy of any publication from the public portal for the purpose of private study or research.
- You may not further distribute the material or use it for any profit-making activity or commercial gain
- You may freely distribute the URL identifying the publication in the public portal -

### Take down policy

If you believe that this document breaches copyright please contact us at [vbn@aub.aau.dk](mailto:vbn@aub.aau.dk) providing details, and we will remove access to the work immediately and investigate your claim.



# Substrate-Insensitive Phased Array with Improved Circularly-Polarized Scan Angle for 5G Mobile Terminals

Shuai Zhang<sup>1</sup>, Igor Syrytsin<sup>1</sup> and Gert Frølund Pedersen<sup>1</sup>

<sup>1</sup> the Department of Electronic Systems, Aalborg University, Denmark (email: sz@es.aau.dk).

**Abstract**— This paper introduces a concept of a substrate-insensitive circularly-polarized phased array for 28 GHz mobile terminal applications. Each array element is a metalized cross slot antenna, which covers the bandwidth of 25-31 GHz. The performance of the designed circularly-polarized antenna is insensitive to substrate permittivity and loss tangent. By adjusting the edge effects of the phased array, the array scan angle with circular polarization can be efficiently improved. User hand effect on the array scan angle with circular polarization is investigated. The proposed mobile terminal phased array is fabricated. S parameters, radiation patterns and realized gain of all the array elements are measured. The measured results agree well with the simulations.

**Index Terms**—mobile antenna, substrate-insensitive antenna, circular polarization, scan angle, 5G application.

## I. INTRODUCTION

As one of the most promising candidates for the fifth generation (5G) communication systems, centimeter-wave (cm-wave)/millimeter-wave (mm-wave) technology has drawn great attentions. In cm-wave/mm-wave cellular communication systems, phased arrays have to be implemented in both mobile terminals and base stations [1] [2]. Different from base stations, phased arrays in mobile terminals may experience frequent change of wireless scenarios due to the mobility of users. It is found in [3] that: in some indoor non-line of sight (NLOS) scenarios at 26 GHz, the channel with both Tx and Rx vertical polarization (VP) can be over 10 dB stronger than the channel with both Tx and Rx horizontal polarization (HP). A typical base station is mounted at a fixed place, which can switch its polarization among VP, HP and circular polarizations. The orientation of a phased array in a mobile terminal varies randomly. It requires the mobile terminal phased array have multiple polarizations. The multiple polarizations can be realized by either reconfigurable dual polarizations or circular polarizations (CP). Reconfigurable polarizations are normally achieved by adding switches or diodes [4]. Currently, the loss of a switch or a diode at 28 GHz is higher than 3 dB, and the price is still high. Furthermore, reconfigurable polarizations will increase the complexity of array feeding or control systems, which will also result in additional losses. CP have the possibility to loss 3 dB if only linear polarization is needed. However, CP solution does not

require any switch or diode, which avoids the loss from switches, diodes and complicated feeding (or controls). In practical applications, it is highly preferred that cm-wave/mm-wave antennas are not sensitive to substrate materials, so that the antennas can be integrated directly on the substrates of different permittivity and losses.

Recently, some works have been carried out on cm-wave/mm-wave antennas for mobile terminals. In [5], the coverage efficiency has been defined to describe the coverage ability of a phased array in space. The coverage efficiency of some phased arrays has been analyzed as well. To further improve the coverage efficiency, a switchable 3D-coverage phased array has been proposed for 5G mobile terminals in [6]. In [7], a phased array has been designed, which can be integrated with FR4 substrate. A switchable dual polarized antenna has been introduced in [8]. However, the designs in [5]-[8] are not circularly polarized. Circularly polarized beam-steering arrays have been investigated in [9] and [10], where the scan angles with circular polarization are around  $\pm 40^\circ$ . However, the antenna performance in [9] and [10] highly depends on the substrate properties.

In this paper, a circularly-polarized phased array operating in the 28 GHz band is proposed for 5G mobile terminals. The performance of the designed circularly-polarized antenna is insensitive to substrate materials. By adjusting the edge effects of the phased array, the array scan angle with circular polarization can be efficiently improved. User hand effect on the circular polarized scan angle of the designed phased array is also investigated. The proposed antenna is fabricated and measured to verify the simulations. All the simulations in this paper are carried out with CST 2016.

## II. ANTENNA CONFIGURATIONS

The configurations of the designed mobile terminal circularly-polarized phased array are shown in Fig. 1. The whole phased array is printed on the 1 mm-thick FR4 substrate with the size of 65 mm  $\times$  130 mm, the relative permittivity of 4.3 and the loss tangent of 0.025. The phased array has 8 antenna elements with the center-to-center distance between the neighboring elements of 6.3 mm. Each element is a metalized cross slot antenna with the substrate material inside the slot removed and the slot inner surface

metalized (see Fig.1 (c)). In this way, the interactions between antenna elements and substrate materials can be minimized. Four inner corners of each metalized cross slot element are chamfered to realize circular polarization. Antenna elements are fed by 50 ohm discrete ports in simulations (see Fig. 1 (c)). The antenna impedance can be changed by  $l_{stub}$ . In order to adjust the edge effects of the phased array, the copper with the size of  $l_b \times w_b$  (on both sides of the PCB) is etched at both ends of the array. The array has bi-directional radiation patterns. In practices, bi-directional radiation patterns are very useful: if one of the two beams is blocked by user tissues, there is still the other beam left for communications. In Fig. 1(b), the copper on the backside of the substrate is only available around the antenna area and the rest of the copper is etched to facilitate the accommodation of electronic components. Furthermore, since slot antennas are easy to excite surface waves on mobile chassis [11], a row of metalized linear slot are placed close to the bottom of the cross slot elements in order to reduce the currents on the backside flowing to the bare FR4 area.

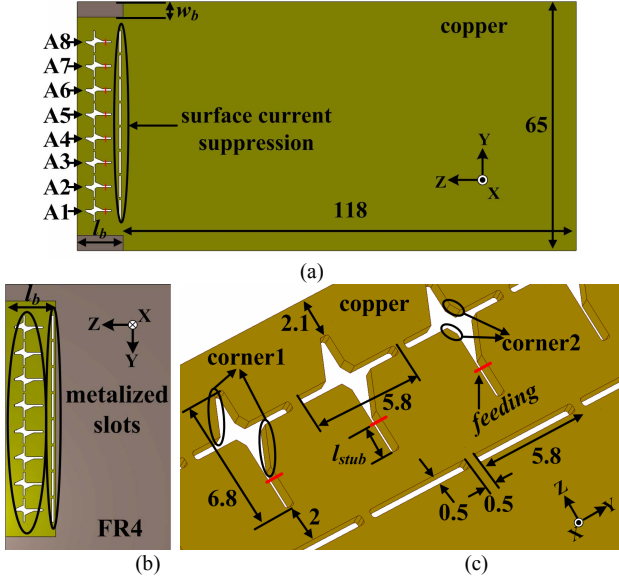


Fig. 1. Antenna geometry: (a) front view, (b) back view, and (c) detailed antenna dimensions in the front view. ( $l_b = 12$ ,  $w_b = 4$ ,  $fd = 4$ ) (Unit: mm)

### III. ANTENNA PERFORMANCE AND ANALYSES

#### A. Impedance Bandwidth and Circular Polarization

The reflection coefficients of the antenna element A2 – A7 (see Fig. 1 (a)) are similar to each other, while those of A1 and A8 are the same. The simulated reflection coefficients of A1 and A4 are shown in Fig. 2. The impedance bandwidth of the antenna elements cover the band of 25-31 GHz. The impedance matching of each elements can be tuned by the stub with the length of  $l_{stub}$  see Fig. 1 (c)). The stub works a quarter-wavelength impedance

transformer. Mutual coupling between array elements are always lower than -15 dB.

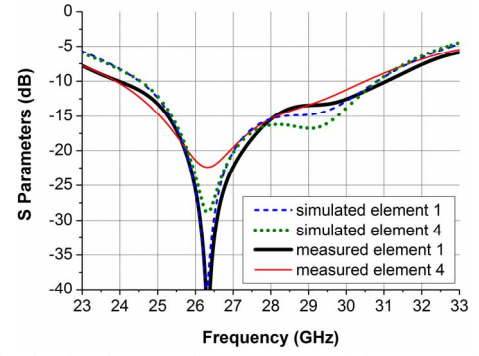


Fig. 2. Simulated and measured S parameters of the antenna element A1 and the antenna element A4.

Circular polarization requires two orthogonal E-field components with the phase difference of  $90^\circ$ . As illustrated in Fig. 3 (a), the two orthogonal E-field components in the proposed antenna are provided by the cross slot, while the  $90^\circ$  phase difference is achieved by changing the dimensions of the four chamfered inner corners ( $l_{a1}$ ,  $Angle1$ ,  $l_{a2}$ ,  $Angle2$ ). For instance, when the designed phased array with all the elements in phase, the main beams of the array point at the directions of  $\phi = 0^\circ$  and  $180^\circ$  (see Fig. 3 (a)). The axial ratio (AR) in the directions of  $\phi = 0^\circ$  and  $180^\circ$  is shown in Fig. 3 (b). By changing  $Angle1$ , the optimal AR in both directions can be obtained simultaneously. In our designed,  $l_{a1}$ ,  $Angle1$ ,  $l_{a2}$ ,  $Angle2$  are optimized to be 2 mm,  $25^\circ$ , 0.5 mm and  $30^\circ$ , respectively. Please note a phased array with the optimal AR in a specific direction cannot guarantee the optimal AR of all the array elements in that direction due to the interactions between the array elements.

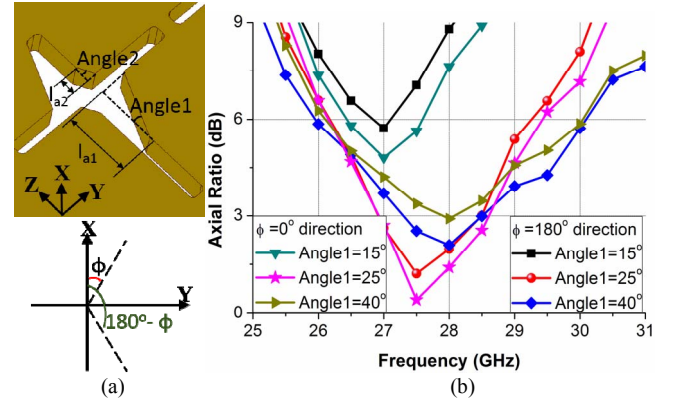


Fig. 3. (a) Single element configurations, (b) axial ratio of the phased array at  $\phi = 0^\circ$  and  $\phi = 180^\circ$ . ( $l_{a1} = 2$ ,  $Angle1 = 25^\circ$ ,  $l_{a2} = 0.5$ ,  $Angle2 = 30^\circ$ ) (Unit: mm)

#### B. Sensitivity of Array Performance to Substrate Materials

In order to study the sensitivity of the array performance to substrate materials, the relative permittivity of the FR4 substrate has been changed from 1 to 10 with the loss tangent of 0.025 the same. The AR and the realized gain of

the array with different substrate permittivity are given in Fig. 4 and Fig. 5, respectively. The AR and realized gain are obtained in the direction of  $\phi = 0^\circ$  and  $180^\circ$ , when all the array elements are in phase. It can be observed that in the  $\phi = 0^\circ$  direction the AR and the realized gain are almost the same under different permittivity. In the  $\phi = 180^\circ$  direction, due to the large bare PCB area (see Fig. 1 (b)), the AR and the realized gain are slightly different but still quite acceptable with the permittivity varying. The loss tangent has also been studied. There is almost no change for both AR and gain, when the loss tangent varies from 0.01 to 1. Therefore, the designed antenna can be integrated on the substrate with different permittivity and loss without changing the antenna performance.

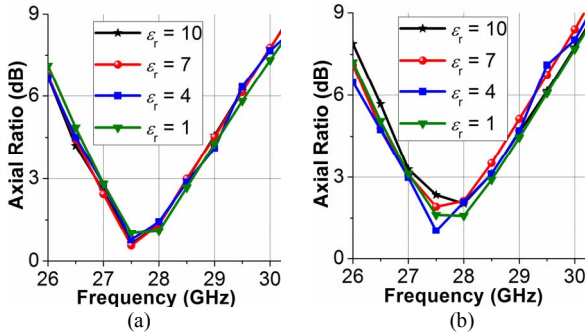


Fig. 4. The axial ratio of the circularly-polarized phase array with different substrate relative permittivity in the direction of (a)  $\phi = 0^\circ$  and (b)  $\phi = 180^\circ$ .

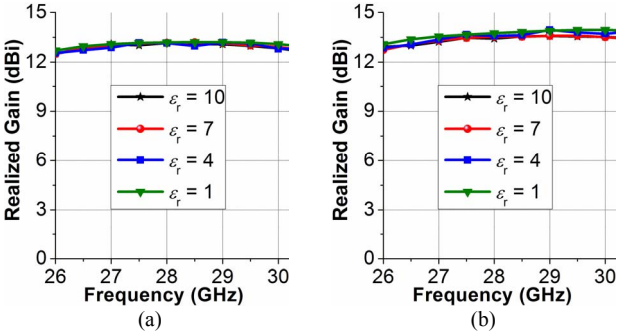


Fig. 5. The realized gain of the circularly-polarized phase array with different substrate relative permittivity in the direction of (a)  $\phi = 0^\circ$  and (b)  $\phi = 180^\circ$ .

### C. Array Scan Angle and Gain with Circular Polarization

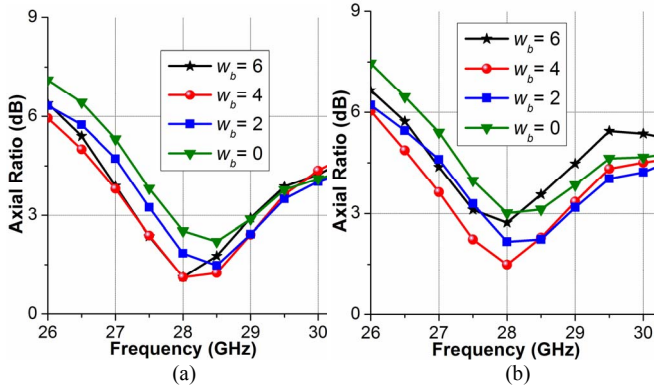


Fig. 6. The axial ratio of the circularly-polarized phase array with different

edge cutting at the direction of (a)  $\phi = 44^\circ$  and (b)  $\phi = 136^\circ$ .

The edges of a linear array have larger effects on the circular polarization of the array when the main beam scans from broadside to larger angle (e.g., from  $\phi = 0^\circ$  to  $\phi = 90^\circ$ ). Fig. 6 shows the AR when the main beam is steered to the direction of  $\phi = 44^\circ$  (and  $\phi = 136^\circ$ ). It is observed that the AR at  $\phi = 44^\circ$  and  $136^\circ$  is already distorted severely without the edge cutting ( $w_b = 0$  mm). By properly etching the part of copper at both ends of the array, the AR at  $\phi = 44^\circ$  and  $136^\circ$  can be optimized. Please note when the main beam is at  $\phi = 0^\circ$  and  $180^\circ$ , the AR at  $\phi = 0^\circ$  and  $180^\circ$  is nearly the same with different  $w_b$ . By utilizing this property, the scan angle of the phased array with circular polarization can be improved efficiently. In Fig. 7, it shows the realized gain and the AR of the array under different main beam directions (of  $\alpha$ ) at 28 GHz. The steered beam can cover the  $\phi$  range of  $-54^\circ$  to  $54^\circ$  and  $126^\circ$  to  $234^\circ$  with circular polarization (AR < 3 dB).

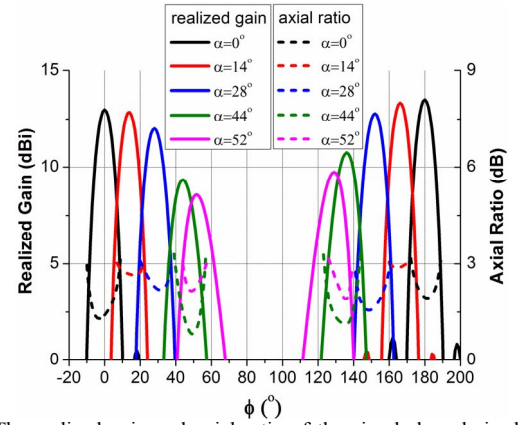


Fig. 7. The realized gain and axial ratio of the circularly-polarized phase array for 5G mobile terminals under different main beam directions at 28 GHz. ( $\alpha$  is the main beam direction)

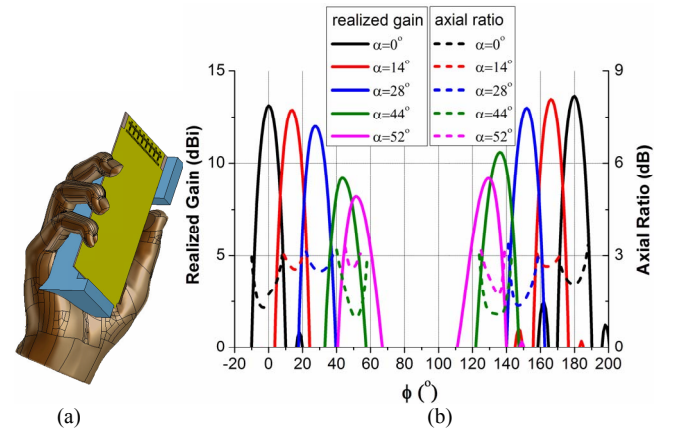


Fig. 8. (a) Simulation setup for the single hand, (b) the realized gain and axial ratio of the circularly-polarized phase array with the user hand under different main beam directions at 28 GHz.

The user hand effects on the array performance are also studied. The proposed phased array is placed on the single



user hand according to the CTIA standard [12] as shown in Fig. 8 (a). The hand tissue has been set as the skin at 28 GHz. In Fig. 8 (b), the realized gain and the AR of the array are also plotted under different main beam directions at 28 GHz. Compared with Fig. 7, it can be clearly observed that the effects of the user hand on the phased array performance is very trivial. This is because the row of metalized linear slot in Fig. 1 mentioned above has reduced the currents on the copper ground plane and the bare FR4 area. The interactions between the CP phased array and the user hand have been minimized.

## II. EXPERIMENTS AND DISCUSSIONS

The proposed antenna are fabricated and the prototype is shown in Fig. 9 (a). Each array element is fed by a 50 ohm thin coaxial cable. To mimic the discrete ports in the simulations, the external surface and the inner pin of a cable are soldered to the two sides of a slot, respectively. The prototype is measured. When one of the antenna elements is under test, all other ports are terminated with 50 ohm loads.

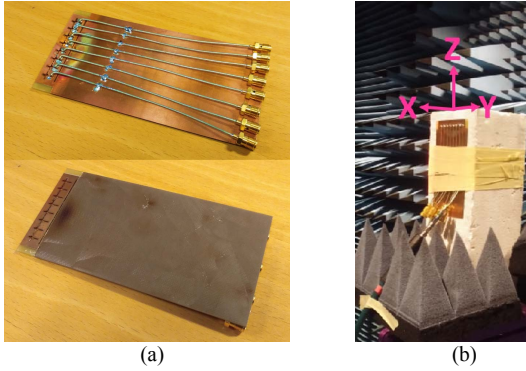


Fig. 9. (a) The prototype of the proposed antenna, and (b) the measurement setups and the coordinate system in a anechoic chamber.

The S parameters of the element A1 and the element A4 (see Fig. 1 (a)) are measured and compared to the simulations in Fig. 2. The measured impedance bandwidth of antenna elements is from 25 to 31 GHz. The measured isolation between the neighboring elements are higher than 14 dB.

The radiation patterns of the array elements are also measured in an anechoic chamber at Aalborg University. The measurement setup and the coordinate system are shown in Fig. 9 (b). The sampling space in the measurement is 5 degree in elevation and 2 degree in the azimuth planes. 11 frequency points have been selected within the frequency range of 27 GHz to 29 GHz. The radiation patterns on xy plane are measured. The radiation patterns of the antenna element A1-A4 at central frequency of 28 GHz are shown in Fig.10. Due to the symmetry antenna configurations only the radiation patterns of A1 to A4 have been provided. In general, the measured and simulated radiation patterns are similar, although the measurements have a little more ripples than the simulations. Measured and simulated realized gain of the element A1 to A4 in the +x axis

direction and -x axis direction is shown in Fig. 11. The measurements align well with the simulations.

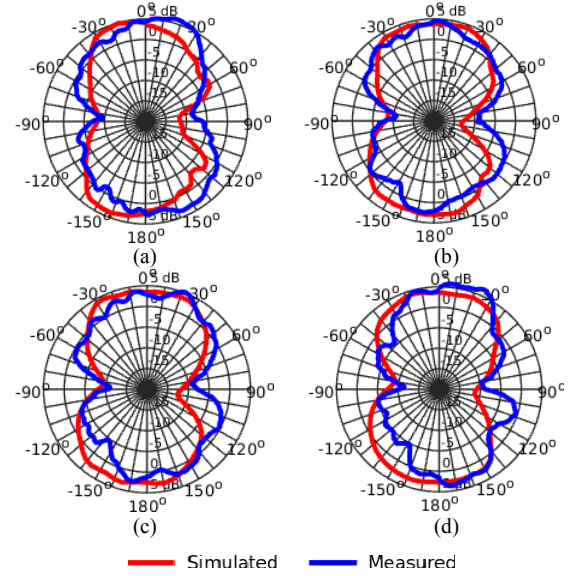


Fig.10. Measured and simulated radiation patterns at 28 GHz on xy plane of the element (a) A1, (b) A2, (c) A3 and (d) A4.

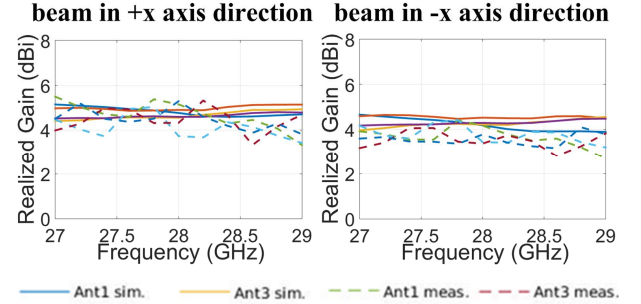


Fig.11. Measured and simulated realized gain of the element A1 to A4 in the +x axis direction and -x axis direction.

## III. CONCLUSIONS

A circularly-polarized phased array has been proposed for 28 GHz mobile terminals. The designed circularly-polarized array is insensitive to substrate properties. The scan angle of the array with circular polarization have been improved by tuning the edge effects. Due to the weak currents flowing on the ground plane (reduced by linear metalized slot), a user hand has very limited effect on the scan angle and the circular polarization. The proposed phased array has been fabricated and measured. The measurements align well with the simulation.

## ACKNOWLEDGMENT

This work was supported by the InnovationsFonden project of RANGE, and also partially supported by Aalborg University Young Talent Program.

## REFERENCES

- [1] T. S. Rappaport, et al., "Millimeter wave mobile communications for 5G cellular: It will work!" *IEEE Access*, vol.1, pp. 335-349, 2013.

- [2] W. Hong, K. -H. Baek, Y. Lee, Y. Kim and S. -T. Ko, "Study and Prototyping of Practically Large-Scale mm Wave Antenna Systems for 5G Cellular Devices," *IEEE communication Magazine*, vol. 52, no. 9, pp. 63-69, 2015.
- [3] J. Ø. Nielsen, and G. F. Pedersen, "Dual-Polarized Indoor Propagation at 26 GHz," *Proceedings of the 27th annual IEEE international symposium on personal, indoor and mobile radio communications*, 2016.
- [4] L. Y. Ji, P. Y. Qin, Y. J. Guo, C. Ding, G. Fu, and S. X. Guo, "A wideband polarization reconfigurable antenna with partially reflective surface," *IEEE Trans. Antennas Propag.*, vol.64, no.10, pp. 4534-4538, 2016.
- [5] J. Helander, K. Zhao, Z. Ying, and D. Sjöberg, "Performance analysis of millimeter wave phased array antennas in cellular handsets," *IEEE Antenna Wireless Propag. Lett.*, vol. 15, 2016.
- [6] N. Ojaroudiparchin, M. Shen, S. Zhang, and G. F. Pedersen, "A switchable 3D-coverage phased array antenna package for 5g mobile terminals," *IEEE Antenna Wireless Propag. Lett.*, vol. 15, pp. 1747-1750, 2016.
- [7] N. Ojaroudiparchin, M. Shen, and G. F. Pedersen, "Investigation on the performance of low-profile insensitive antenna with improved radiation characteristics for the future 5G applications," *Microwave and Optical Technology Letter*, vol. 58, no. 9, pp. 2148-2151, 2016.
- [8] W. Hong, S. -T. Ko,, Y. Lee, and K. -H. Baek, "Multi-polarized antenna array configuration for mmWave 5G mobile terminals," *The 2015 International Workshop on Antenna Technology*, 2015.
- [9] C. Liu, S. Xiao, Y. X. Guo, M.-C. Tang, Y. Y. Bai, and B.-Z. Wang, "Circularly polarized beam-steering antenna array with butler matrix network," *IEEE Antennas Wireless Propag. Lett.*, vol. 10, pp.1278–1281, 2011.
- [10] N. B. Buchanan, V. F. Fusco, et al, "A circular polarized self-tracking l band array with high bandwidth and scan beamwidth for Inmars at BGAN applications," in *Proc. 5th Eur. Conf. on Antennas Propag. (EUCAP)*, pp. 211–215, 2011.
- [11] S. Zhang, X. Chen, I. Syrytsin, and G. F. Pedersen, "A planar switchable 3D-coverage phased array antenna and its user effects for 28 GHz mobile terminal applications" *IEEE Trans. Antennas Propag.* (submitted)
- [12] Test plan for Mobile Station Over the Air Performance CTIA revision 3.1, Jan. 2011.